Hindawi Publishing Corporation
Journal of Nanomaterials
Volume 2013, Article ID 404210, 9 pages
http://dx.doi.org/10.1155/2013/404210

Research Article

Fabrication of Pamidronic Acid-Immobilized TiO_2/Hydroxyapatite Composite Nanofiber Mats for Biomedical Applications

Yong-Suk Shin,[1] Jyoti S. Borah,[1] Adnan Haider,[1] Sukyoung Kim,[2] Man-Woo Huh,[3] and Inn-Kyu Kang[1]

[1] *Department of Polymer Science & Engineering, Kyungpook National University, Daegu 702-701, Republic of Korea*
[2] *School of Materials Science and Engineering, Yeungnam University, Gyeongbuk 714-729, Republic of Korea*
[3] *School of Textile and Fashion Technology, Kyungil University, Kyungsan 712-701, Republic of Korea*

Correspondence should be addressed to Inn-Kyu Kang; ikkang@knu.ac.kr

Received 14 October 2013; Accepted 29 November 2013

Academic Editor: Zhongkui Hong

TiO_2/hydroxyapatite (TiO_2/HA) composite nanofiber mats were fabricated using an electrospinning technique. Subsequently, pamidronic acid (PDA) was immobilized on the surface of the TiO_2/HA nanofiber mat to improve osseointegration. X-ray photoelectron microscopy and scanning electron microscopy (SEM) were used to characterize the structure and morphology of the PDA-immobilized TiO_2/HA composite nanofiber mat (TiO_2/HA-P). The potential of TiO_2/HA-P as a bone scaffold was assessed by examining the cell adhesion and proliferation of osteoblasts and osteoclasts. The adhesion and proliferation of osteoblasts on the TiO_2/HA-P composite nanofiber mat were slightly higher than those on the TiO_2/HA composite nanofiber mat, whereas the viability of osteoclasts on the TiO_2/HA-P nanofiber mat was significantly suppressed. These results suggest that the TiO_2/HA-P nanofiber mat has the potential for use as a therapeutic bone implant.

1. Introduction

Titanium (Ti) and some of its alloys are the most widely used metallic materials for biomedical applications. Their inherent biocompatibility, excellent mechanical properties, and corrosion resistance make them suitable for biomaterials in tissue engineering [1, 2]. Over the past few decades, a range of materials and designs have been used to improve the osseointegration of titanium implants [3–7]. Hydroxyapatite (HA), a major inorganic component of natural bone and teeth, has been studied extensively and used in biomedical implant applications and bone regeneration owing to its good osteoconductivity and bone binding ability to natural bone [8–11]. The addition of hydroxyapatite (HA) to titanium implants has attracted considerable interest because of its potential use as a biomaterial with a range of treatments, such as sol-gel and hydrolysis and hydrothermal treatment [12]. Many researchers have examined TiO_2/HA composites [13, 14]. Ramires et al. investigated the biocompatibility of TiO_2/HA composite coatings and reported that they are bioactive and effective in improving the growth of osteoblasts [15]. Bigi et al. reported that hydroxyapatite-coated nanostructured titanium alloys induce the differentiation of mesenchymal cells (MSCs) towards a phenotypic osteoblast lineage [16]. Recently Kim et al. prepared TiO_2/HA composite nanofiber mats using an electrospinning technique and immobilized collagen on the surface of the mats to improve the tissue compatibility. They showed that the collagen-immobilized TiO_2/HA composite nanofiber mats induced better adhesion, proliferation, and differentiation of osteoblasts than the unmodified TiO_2/HA composites [17].

The surface properties of implanted materials play important roles in tissue acceptance and cell survival. Over the last few decades, a range of techniques and materials with surface modifications have been developed to improve the biological surface properties of implant materials [18–20]. Pamidronic

acid, a nitrogen containing bisphosphonate, has recently gained importance as a surface modifier for orthopedic and dental implants. PDA is used to prevent bone loss and treat osteoporosis in a variety of diseases, such as bone metastasis, hypercalcemia of a malignancy, and Paget's disease [21–24]. In orthopedic implants, PDA is expected to inhibit the bone resorptive activity of osteoclasts, thereby promoting osteogenesis at the bone tissue/implant interface [25, 26]. Yoshinari et al. reported that PDA-immobilized titanium has no cytotoxic effects on osteoblasts and affects the differentiation of osteoblasts [27]. Kajiwara et al. reported that a PDA-immobilized titanium surface stimulates new bone formation around the implant *in vivo*, which contributes to the success of implant technology [28]. A previous study showed that PDA-immobilized titanium nanotube suppressed the viability of osteoclasts and reduced their bone resorption activity [29]. On the other hand, there are no reports on the immobilization of PDA on TiO_2/HA composite nanofiber mats. The combination of TiO_2, HA, and PDA in the scaffolds should have combined benefits that are not achieved by the individual components.

In this study, TiO_2/HA composite nanofiber mats were prepared using an electrospinning method. Pamidronic acid was then immobilized onto the surface of the nanofiber composite mats. Its potential use in bone regeneration and tissue engineering was examined by comparing the *in vitro* cellular response to the surface-modified (TiO_2/HA-P) and unmodified (TiO_2/HA) composite nanofiber mats in terms of cell adhesion and proliferation.

2. Experimental

2.1. Materials. Titanium isopropoxide, pamidronic acid, calcium nitrate tetrahydrate, polyvinylpyrrolidone (PVP), tetraethylorthosilicate (TEOS), 2-methoxyethanol, Poly (ethylene glycol) bis (carboxymethyl) ether (molecular weight (Mn) 250) (PEG), carbodiimide, isopropanol, aqueous formaldehyde, (tetramethylrhodamine isothiocyanate)-phalloidin (TRICK) were purchased from Sigma Aldrich. Phosphate buffer saline (PBS), 3-(4,5-dimethylazol-2-yl)-2,5-diphenyl-2H-tetrazolium bromide assay (MTT), Dulbecco's Modified Eagle Medium (DMEM), fetal bovine serum (FBS), penicillin streptomycin (PGS) were purchased from Gibco, Invitrogen, USA, tartrate-resistant phosphatase (TRAP) staining kit was purchased from Kamiya Biomedical Company, Seattle, WA USA, and 4′,6-diamidino-2-phenylindole (DAPI) was purchased from Millipore. All the chemicals were used without further purification.

2.2. Methods

2.2.1. Solution Preparation. HA and TiO_2 solutions were prepared according to the literature protocols [13, 17]. Briefly, a HA solution was prepared by vigorously stirring a mixture of precursors, such as calcium nitrate tetrahydrate and triethyl phosphate in 2-methoxyethanol. First, calcium nitrate tetrahydrate (4.0 g, 1 M) and triethyl phosphate (1.86 g, 0.6 M) were hydrolyzed at room temperature for 24 h in a beaker containing 2-methoxyethanol and distilled water, respectively. Both precursors were mixed at a Ca/P ratio of 1.67 with vigorous stirring for 5 h at room temperature. For aging, the as-prepared precursors were closely capped and placed in an oven at 37°C for 7 days. A HA solution with the appropriate viscosity was obtained via a slow evaporation process of the precursor at 40°C for 48 h. To produce the TiO_2 solution, titanium isopropoxide (1 M) was hydrolyzed in a 2-methoxyethanol solution, and polyvinylpyrrolidone (PVP) (8–13 wt%) was then added to the TiO_2-methoxyethanol solution as a binding agent. The mixed solutions were then stirred at room temperature for 24 h to obtain a TiO_2/PVP solution. Subsequently, 2 wt% HA solution and 1 wt% tetraethylorthosilicate (TEOS) were mixed with the TiO_2/PVP solution to prepare a TiO_2/PVP/HA solution. The mixed solution was stirred vigorously at room temperature for 6 h and then slowly for further 3 h at 40°C to achieve the appropriate viscosity and electroconductivity for the electrospinning process.

2.2.2. Fabrication of TiO_2/HA Composite Nanofiber Mats. TiO_2/PVP/HA solutions prepared above were then subjected to electrospinning. The electrospinning experiments were carried out at room temperature, and the apparatus for electrospinning was assembled based on the study reported by Lee et al. [30]. The TiO_2/PVP/HA solution was filled in a 10 mL glass syringe fitted with a needle with an inner diameter of 0.4 mm. The jets generated from the needle by high voltage flew to the collector and formed a nanofiber mat. The TiO_2/PVP/HA solutions were electrospun under a range of conditions with a mass flow rate of 0.5–1.0 mL/h, applied voltage between 10 and 20 kV, a tip to collector distance of 10–20 cm, and solution concentration from 8 to 13 wt %. The electrospun samples were dried overnight at 40°C to remove moisture and were cut into 10 cm^2 pieces of nanofiber mat. The as-spun TiO_2/PVP/HA nanofiber mats were then calcined at 800°C for 3 h at a very low heating rate (1°C/min) to completely eliminate PVP from the nanocomposite. The calcined TiO_2/HA composite nanofiber mats were used for PDA immobilization. The morphology of the TiO_2/HA composite nanofiber mats was observed by field emission scanning electron microscopy (FE-SEM, Jeol Co., JSM 6700F). The calcined TiO_2/HA nanofibers were crushed and dispersed in distilled water. The dispersed nanofiber fragments were collected on carbon-coated copper grids (300 mesh) and observed by transmission electron microscopy (TEM, H-7600, Hitachi Ltd.).

2.2.3. Immobilization of Pamidronic Acid (PDA) on TiO_2/HA Composite Nanofiber Mats. The immobilization of PDA on the TiO_2/HA composite nanofiber mats was carried out in three steps. First, the primary amine ($-NH_2$) group was introduced to the surface of the TiO_2/HA composite nanofiber mats by a reaction of aminopropyltriethoxysilane (APTES) with surface hydroxyl group (–OH) of TiO_2/HA composite nanofiber mats. Poly (ethylene glycol) bis (carboxymethyl) ether was activated with water soluble carbodiimide and reacted with the free terminal amino groups of TiO_2/HA

composite nanofiber mats to produce terminal carboxylic acid on the surface. PDA was then immobilized using the free terminal carboxyl groups of the mats to prepare PDA-immobilized TiO_2/HA composite nanofiber mats. Briefly, a TiO_2/HA composite nanofiber mat ($6 \times 6\ cm^2$) was immersed in an APTES-water solution (1 : 9) and sonicated for 30 min. The nanofiber mats were then heated to 90°C for 2 h with gentle stirring. The silanized TiO_2/HA composite nanofiber mats were washed with water in an ultrasonic cleaner and dried under reduced pressure and room temperature to produce the primary amine-coupled TiO_2/HA composite nanofiber mats (TiO_2/HA-A). The TiO_2/HA-A nanofiber mat was then immersed in a beaker containing an aqueous solution of poly (ethylene glycol) bis (carboxymethyl) ether (10^{-5} M, 100 mL) and a WSC solution of (1-ethyl-3-(3-dimethylaminopropyl) carbodiimide hydrochloride (EDC, 0.5 g; 0.25 wt%) and N-hydroxysuccinimide (NHS, 0.5 g; 0.25 wt%) dissolved in 20 mL water) and it was stirred gently for 5 h at 4°C followed by alkaline hydrolysis to obtain the carboxyl functional TiO_2/HA composite nanofiber mat (TiO_2/HA-C). Terminal carboxylic acid of TiO_2/HA-C was then activated with water soluble carbodiimide and immersed in a solution of pamidronic acid sodium salt hydrate and stirred for 12 hr at 4°C to obtain the PDA-immobilized TiO_2/HA composite nanofiber mats (TiO_2/HA-P, Figure 1). TiO_2/HA-P was then washed with distilled water and dried. PEG was used due to its long chain that will help in dynamic motion and improved flexibility of the molecules. Thus it will prompt interaction of osteoblasts and osteoclasts with TiO_2/HA-P and TiO_2/HA composite nanofiber mats. The chemical composition of the TiO_2/HA-P surface was analyzed by electron spectroscopy for chemical analysis (ESCA, ESCA LAB VIG Microtech, East Grinstead, UK) using MgKα radiation at 1253.6 eV and a 150 W power mode at the anode.

2.2.4. Osteoblastic Cell Culture. To examine the interaction of the TiO_2/HA-P and TiO_2/HA composite nanofiber mat with osteoblasts (MC3T3-E1), the nanofiber composite mats were cut into small circular discs, fitted inside a 24-well culture dish, and immersed in a Dulbecco's Modified Eagle Medium (DMEM) containing 10% fetal bovine serum (FBS). Subsequently, 1 mL of the MC3T3-E1 cell solution (3×10^4 cells/mL) was added to the surface of the nanofiber composite mats and incubated in a humidified atmosphere containing 5% CO_2 at 37°C for 1 and 2 days. After incubation, the supernatant was removed, and the nanofiber composite mats were washed twice with phosphate buffered saline (PBS) and fixed in a 4% formaldehyde aqueous solution for 15 min. The samples were then dehydrated, dried in a critical-point drier, and sputter-coated with gold. The surface morphology of the nanofiber composite mats was observed by FE-SEM.

A 3-(4,5-dimethylazol-2-yl)-2,5-diphenyl-2H-tetrazolium bromide (MTT) assay was used to determine the proliferation of osteoblasts on the TiO_2/HA-P and TiO_2/HA composite nanofiber mats. Briefly, MC3T3-E1 osteoblasts were seeded at a concentration of 3×10^4 cells/mL on the TiO_2/HA and TiO_2/HA-P composite nanofiber mats, which were fitted in a 24-well plate, and cell proliferation was monitored after 1 and 3 days of incubation. A MTT solution (50 μL, 5 mg/mL in PBS) was added to each well and incubated in a humidified atmosphere containing 5% CO_2 at 37°C for 4 hrs. After removing the medium, the converted dye was dissolved in acidic isopropanol (0.04 N HCl-isopropanol) and kept in the dark at room temperature for 30 min. From each sample, the medium (100 μL) was taken, transferred to a 96-well plate, and subjected to ultraviolet measurements for the converted dye at a wavelength of 570 nm on a kinetic microplate reader (EL x 800, Bio-T Instruments, Inc, Highland Park, USA).

2.2.5. Differentiation of Macrophage. For osteoclastic differentiation, the hematopoietic stem cells (HSC, RAW 264.7) at a cell density of 3×10^4 cells/mL were cultivated on TiO_2/HA-P and TiO_2/HA composite nanofiber mats in a DMEM medium containing 10% FBS, 50 ng/mL mouse recombinant receptor activator of nuclear factor Kappa-B ligand (RANKL), and 50 ng/mL macrophage colony-stimulating factors from mouse (m-CSF). The culture medium was changed every 2 days.

2.2.6. Tartrate-Resistant Phosphatase (TRAP) Staining and Solution Assays. To analyze the osteoclastic differentiation, the cells after 3 days of culture in the differentiation medium were washed once with PBS and fixed with 10% formalin (50 μL, neutral buffer) at room temperature for 5 min. After fixation, the cells were washed with distilled water and incubated with a substrate solution (3 mg of chromogenic substrate with 5 mL tartrate containing buffer (pH 5.0)) for 30 min at 37°C. The cell images were obtained by fluorescence microscopy (Carl Zeiss, Axioplan 2, Germany).

For immunocytochemistry, the HSC were cultivated in a differentiation medium. After 4 days, they were fixed and immunostained after 4 days with 4′,6-diamidino-2-phenylindole (DAPI) and {(tetramethylrhodamine isothiocyanate)-phalloidin} (TRICK) as described previously [31]. Multinucleated cells containing more than three nuclei were considered differentiated osteoclast-like cells. The cell images were obtained by fluorescence microscopy.

To examine the viability of the osteoclast cells on the TiO_2/HA and TiO_2/HA-P composite nanofibers mats, the differentiated macrophage cells after 3 days of culture were stained with calcein-AM and propidium iodide. The differentiated macrophages cells were suspended in PBS with a cell density of $1 \times 10^5 - 1 \times 10^6$ cells/mL. Subsequently, 200 μL of a cell suspension was mixed with a 100 μL assay solution and incubated for 15 min at 37°C. The assay solution composition was; 10 μL calcein-AM solution (1 mM in dimethyl sulfoxide (DMSO)), and 5 μL propidium iodide (1.5 mM in H_2O) was mixed with 5 mL PBS. The cells were examined by fluorescence microscopy with excitation at 490 nm for the simultaneous monitoring of viable and dead cells.

The proliferation of differentiated macrophages cells on the TiO_2/HA-P and TiO_2/HA composite nanofiber mat was assessed using a 3-(4,5-dimethylazol-2-yl)-2,5-diphenyl-2H-tetrazolium bromide (MTT) assay, as described in the section for the osteoblastic cell culture, and examined by fluorescence microscopy.

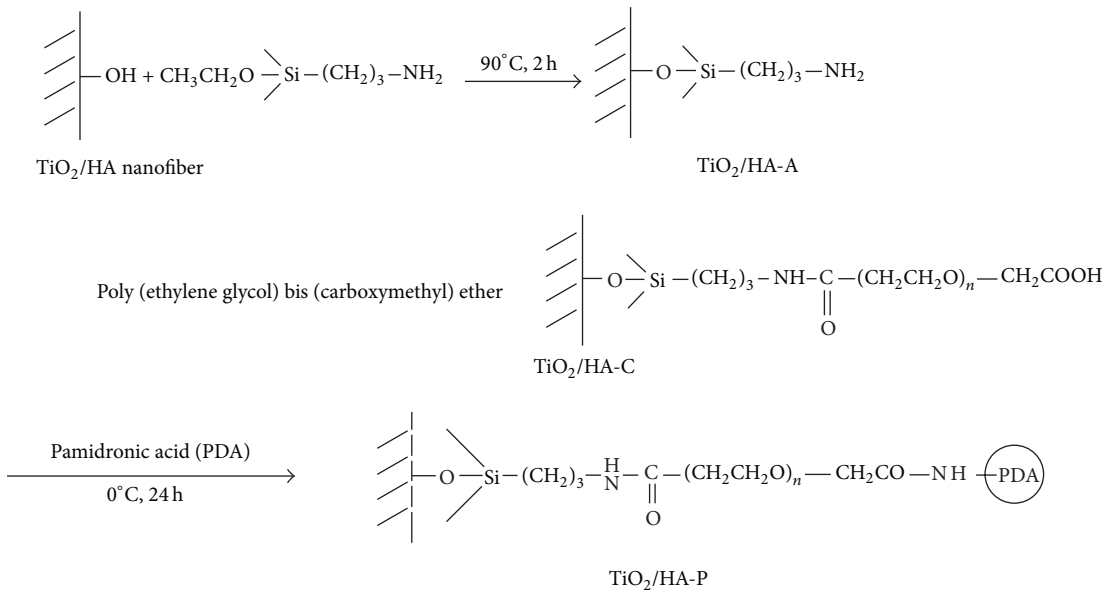

Figure 1: Schematic diagram of the production of the PDA-immobilized TiO_2/HA composite nanofiber mats.

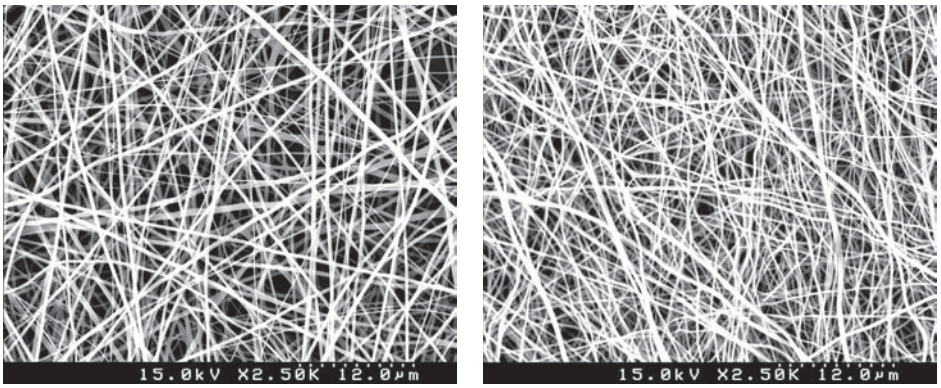

(a) (b)

Figure 2: FE-SEM images of the TiO_2/HA composite nanofiber mats (a) before heat treatment and (b) after heat treatment.

3. Results and Discussion

3.1. Surface Characterization of the TiO_2/HA Composite Nanofiber Mats. The surface morphology of the TiO_2/HA composite nanofiber mat (before and after calcination at 800°C for 3 h) was examined by FE-SEM. As can be observed from the FE-SEM images depicted in Figure 2, the morphology of the TiO_2/HA composite nanofiber before and after calcinations was uniform and beadless. After calcinations the heat treated nanofibers showed no drastic morphological change apart from the fact that there was decrease in the TiO_2/HA composite nanofiber diameter because of the decomposition of PVP at elevated temperature, which was used as a binding source. After calcinations the calculated outer mean diameter of the nanofibers was 100 nm.

The morphology of the TiO_2/HA nanofiber was further assessed by TEM. Figure 3(a) shows TEM micrograph of a free standing TiO_2/HA nanofiber having average diameter slightly above 100 nm. The fiber surface is smooth and uniform, which indicates that TiO_2 was uniformly dispersed in the PVP mixture. The fibers were uniform and consisted of grains which were densely packed along the fiber length. Figure 3(b) is the magnified TEM micrograph of the TiO_2/HA composite nanofiber.

3.2. Immobilization of PDA on TiO_2/HA Composite Nanofiber Mats. The immobilization of PDA on the TiO_2/HA composite nanofiber mats was confirmed by ESCA (Figure 4). The N1s and P2p photoelectron signal is the marker of choice for confirming successful PDA immobilization. The TiO_2/HA composite nanofiber mat (Figure 4(a)) showed three photoelectron signals corresponding to C1s (binding energy, 285 eV), Ti2p3 (binding energy, 459 eV), and O1s (binding energy, 529 eV). On the other hand, seven photoelectron signals were observed for TiO_2/HA-P (Figure 4(c)), which corresponds to C1s, Ti2p3, O1s, N1s (binding energy,

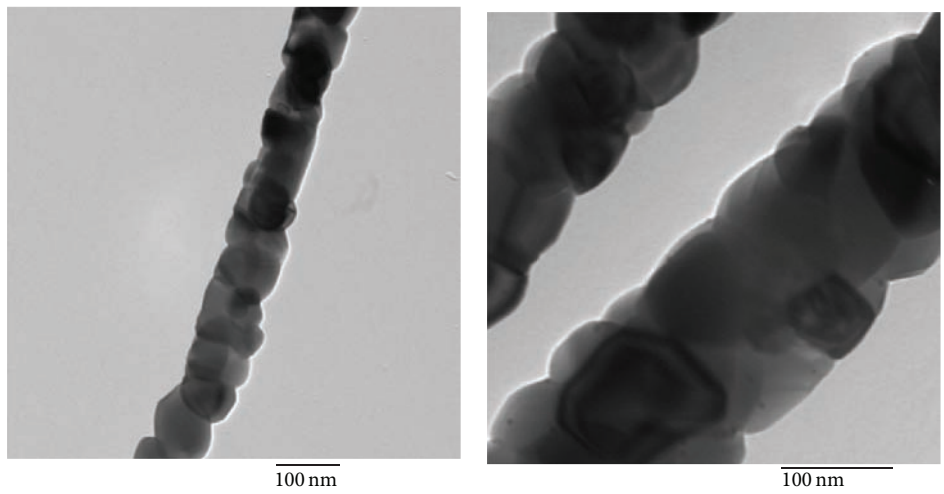

Figure 3: TEM images of (a) TiO_2/HA nanofiber (magnification: ×15,000) and (b) high resolution (magnification: ×40,000).

Table 1: Chemical composition of the surface-modified TiO_2/HA nanofibers calculated from the survey scan spectra.

Substrate	Atomic %					
	C	O	Ti	N	Si	*P*
TiO_2/HA	21.2	55.8	18.3	0.1	1.3	<0.1
TiO_2/HA-A	49.1	31.0	3.5	4.1	12.3	<0.1
TiO_2/HA-P	49.0	33.5	7.6	5.8	2.5	0.8

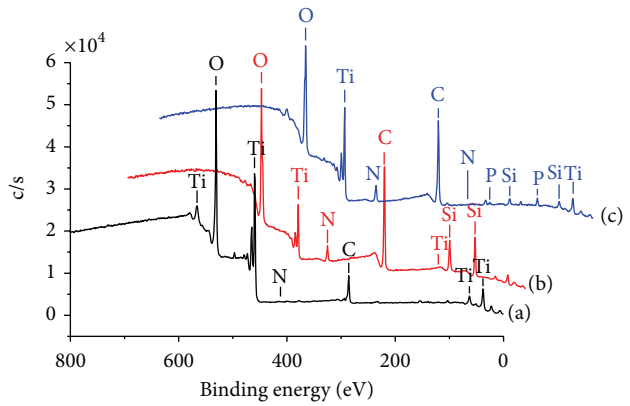

Figure 4: ESCA spectra of (a) TiO_2/HA, (b) TiO_2/HA-A, and (c) TiO_2/HA-P nanofiber mats.

401 eV), Si2s (binding energy, 154 eV), and P2p (binding energy, 133.7 eV). The binding energies of the N1s and P2p photoelectrons obtained from TiO_2/HA-P were assigned to NH_2^- (400.6–401.9 eV) and PO_4^{-3} (133.7), respectively [32]. The presence of two new elements, N and P, in TiO_2/HA-P confirmed the immobilization of PDA on the surface of the TiO_2/HA composite nanofiber mat. Table 1 lists the elements calculated from the scan spectra of the mats.

4. Interaction of Bone Cells with TiO_2/HA-P and TiO_2/HA Composites Nanofiber Mats

4.1. Adhesion and Proliferation of Osteoblasts. The *in vitro* osteoblastic cells behavior on the TiO_2/HA-P and TiO_2/HA composite nanofiber mats was examined in terms of cell adhesion and cell proliferation. Figure 5 depicts SEM images of the osteoblastic cells adhered to the surface of the TiO_2/HA and TiO_2/HA-P mats after 1 and 2 days of culture. Regardless of the type of mat, the number of adhered cells increased with time. Slightly more cells adhered to TiO_2/HA-P than TiO_2/HA, but the differences were not significant.

Comparative studies for the proliferation of osteoblasts and osteoclasts were carried out by using MTT assay. Figure 6 represents the results of the MTT assay of osteoblastic cells cultured on TiO_2/HA-P and TiO_2/HA composite nanofiber mats after 1 and 3 days of culture. The proliferation of osteoblastic cells cultured on TiO_2/HA-P composites nanofiber mat was slightly higher than that on TiO_2/HA composite nanofiber mat, indicating that PDA immobilization was not toxic to osteoblasts, highlighting the favorable microenvironment for osteogenetic ability.

4.2. Differentiation of Macrophages into Osteoclasts and Viability on the Nanofiber Mats. To examine the viability of osteoclast cells, the hematopoietic stem cells (HSC) from mice were seeded on an unmodified TiO_2/HA and TiO_2/HA-P composite nanofiber mats and induced to differentiate

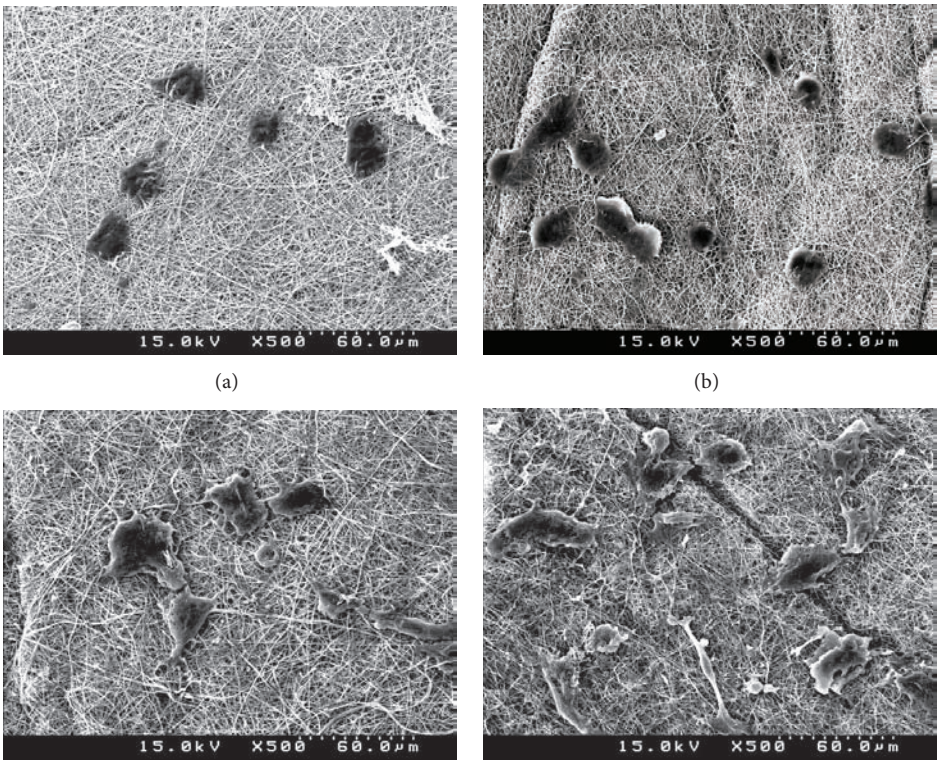

Figure 5: FE-SEM images of osteoblasts adhered to TiO_2/HA ((a), (c)) and TiO_2/HA-P ((b), (d)) nanofiber mats after 1 day ((a), (b)) and 2 days ((c), (d)).

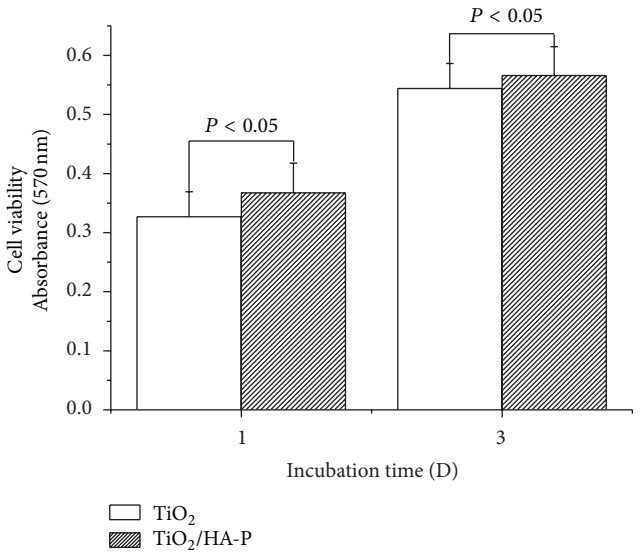

Figure 6: MTT assay with absorbance as a measure of osteoblast proliferation. The cells were cultured on TiO_2/HA and TiO_2/HA-P for different culture times.

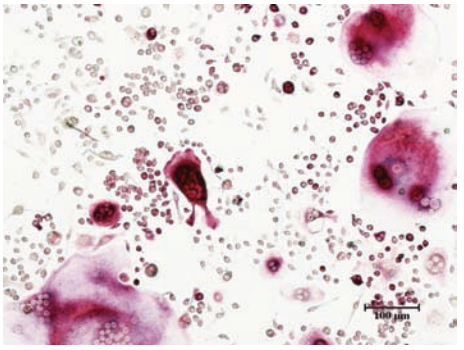

Figure 7: Identification of osteoclasts by TRAP staining (red colored cells are osteoclasts).

into multinucleated osteoclasts-like cells using standard m-CSF and RANKL procedures [29]. The differentiation of macrophage cells into osteoclasts was confirmed using a series of staining agents. TRAP is a marker of osteoclasts and shows a red color when stained with a tartrate and chromogenic substrate. After 3 days of differentiation, TRAP positive cells were observed, indicating that the macrophages had differentiated into osteoclasts (Figure 7).

The differentiated macrophage stained with calcein-AM and propidium iodide exhibited green fluorescence on the TiO_2/HA composite nanofiber mat, indicating the good viability of the cells (Figure 8(a)). On the other hand, in addition to the green fluorescence, red fluorescence was also observed on the TiO_2/HA-P composite nanofiber mat,

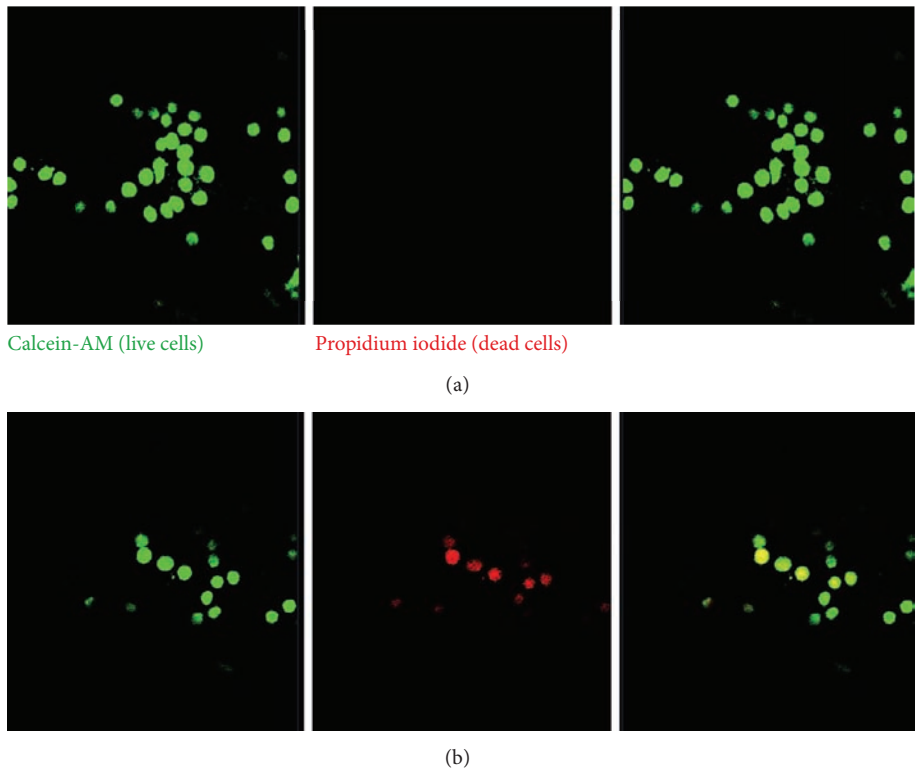

FIGURE 8: Fluorescence microscopy images of calcein-AM (green) and propidium iodide (red) marked differentiated macrophages on (a) TiO_2/HA and (b) TiO_2/HA-P after 3 days culture (magnification: ×200).

suggesting that some osteoclast cells died when they came in contact with PDA (Figure 8(b)).

Figure 9 illustrates the MTT assay of the osteoclasts cultured onto TiO_2/HA and TiO_2/HA-P composite nanofiber mats surface after 3 and 4 days of culture. The level of osteoclasts proliferation on the TiO_2/HA-P composite nanofiber mat was significantly lower than that on the TiO_2/HA composite nanofiber mat. Osteoclasts normally destroy themselves by apoptosis, a form of cell suicide. PDA encourages osteoclasts to undergo apoptosis by binding and blocking the enzyme, farnesyl diphosphate synthase (FPPS), in the mevalonate pathway [33]. Therefore, PDA immobilized on the TiO_2/HA composite nanofiber mat suppressed the viability of the osteoclasts and has the potential to reduce their bone resorption activity. These results suggested that TiO_2/HA-P composite nanofiber mats hold this unique property of reducing osteoclast cells growth and at the same time providing favourable environment for the osteoblast cells proliferation (Figure 6).

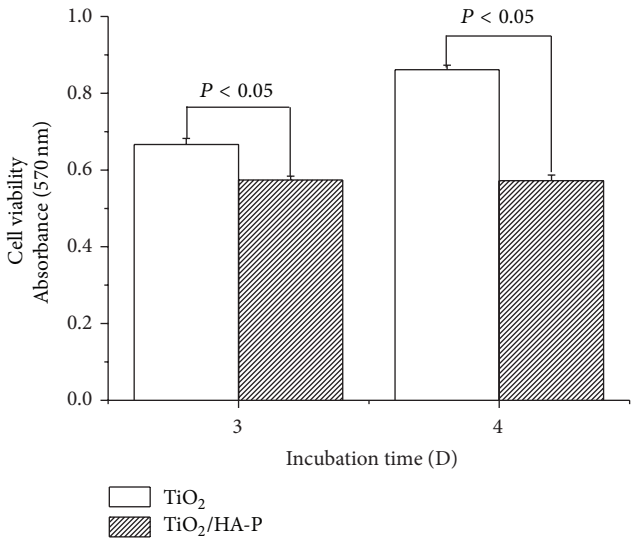

FIGURE 9: MTT assay, absorbance as a measure of cell proliferation of osteoclasts cultured on TiO_2/HA and TiO_2/HA-P nanofiber mats for different culture time.

5. Conclusion

TiO_2/HA composite nanofiber mats were prepared by an electrospinning technique and pamidronic acids were immobilized on the surface of the mat. PDA immobilized on the TiO_2/HA composite nanofiber mats did not show any cytotoxicity on the osteoblast cells. On the other hand, the viability of the osteoclasts was suppressed on the PDA-immobilized TiO_2/HA composite nanofiber mat. From these results it is concluded that TiO_2/HA-P nanofiber mat has strong potential for use as a therapeutic bone implant.

Authors' Contribution

Yong-Suk Shin, Jyoti S. Borah, Adnan Haider, Sukyoung Kim, Man-Woo Huh, and Inn-Kyu Kang contributed equally to this work.

Acknowledgments

This study was supported by the Kyungpook National University Research Fund, 2013, and General Research Program (2013 RIA 2005148) from the Ministry of Education, Science and Technology of Korea.

References

[1] Y. Liu, J. P. Li, E. B. Hunziker, and K. De Groot, "Incorporation of growth factors into medical devices via biomimetic coatings," *Philosophical Transactions of the Royal Society A*, vol. 364, no. 1838, pp. 233–248, 2006.

[2] C. N. Elias, J. H. C. Lima, R. Valiev, and M. A. Meyers, "Biomedical applications of titanium and its alloys," *JOM*, vol. 60, no. 3, pp. 46–49, 2008.

[3] H. W. Kim, Y. H. Koh, L. Li, H. S. Lee, and H. E. Kim, "Hydroxyapatite coating on titanium substrate with titania buffer layer processed by sol-gel method," *Biomaterials*, vol. 25, no. 13, pp. 2533–2538, 2004.

[4] S. Tamilselvi, H. B. Raghavendran, P. Srinivasan, and N. Rajendran, "In vitro and in vivo studies of alkali- and heat-treated Ti-6Al-7Nb and Ti-5Al-2Nb-1Ta alloys for orthopedic implants," *Journal of Biomedical Materials Research A*, vol. 90, no. 2, pp. 380–386, 2009.

[5] J. Guo, R. J. Padilla, W. Ambrose, I. J. De Kok, and L. F. Cooper, "The effect of hydrofluoric acid treatment of TiO_2 grit blasted titanium implants on adherent osteoblast gene expression in vitro and in vivo," *Biomaterials*, vol. 28, no. 36, pp. 5418–5425, 2007.

[6] T. Albrektsson, P.-I. Branemark, H.-A. Hansson, and J. Lindstrom, "Osseointegrated titanium implants. Requirements for ensuring a long-lasting, direct bone-to-implant anchorage in man," *Acta Orthopaedica Scandinavica*, vol. 52, no. 2, pp. 155–170, 1981.

[7] D. Gong, C. A. Grimes, O. K. Varghese et al., "Titanium oxide nanotube arrays prepared by anodic oxidation," *Journal of Materials Research*, vol. 16, no. 12, pp. 3331–3334, 2001.

[8] L. L. Hench, "Bioceramics: from concept to clinic," *Journal of the American Ceramic Society*, vol. 74, no. 7, pp. 1487–1510, 1991.

[9] M. M. A. Ramselaar, F. C. M. Driessens, W. Kalk, J. R. De Wijn, and P. J. Van Mullem, "Biodegradation of four calcium phosphate ceramics; in vivo rates and tissue interactions," *Journal of Materials Science*, vol. 2, no. 2, pp. 63–70, 1991.

[10] F. Wang, M. S. Li, Y. P. Lu, Y. X. Qi, and Y. X. Liu, "Synthesis and microstructure of hydroxyapatite nanofibers synthesized at 37 ◦c," *Materials Chemistry and Physics*, vol. 95, no. 1, pp. 145–149, 2006.

[11] H. W. Kim and H. E. Kim, "Nanofiber generation of hydroxyapatite and fluor-hydroxyapatite bioceramics," *Journal of Biomedical Materials Research B*, vol. 77, no. 2, pp. 323–328, 2006.

[12] H. Anmin, L. Tong, L. Ming, C. Chengkang, L. Huiqin, and M. Dali, "Preparation of nanocrystals hydroxyapatite/TiO_2 compound by hydrothermal treatment," *Applied Catalysis B*, vol. 63, no. 1-2, pp. 41–44, 2006.

[13] H. W. Kim, H. E. Kim, V. Salih, and J. C. Knowles, "Hydroxyapatite and titania sol-gel composite coatings on titanium for hard tissue implants; mechanical and in vitro biological performance," *Journal of Biomedical Materials Research B*, vol. 72, no. 1, pp. 1–8, 2005.

[14] X. Jin, Y. Guo, J. Wang et al., "The preparation of TiO_2/hydroxylapatite (TiO_2/HA) composite and sonocatalytic damage to bovine serum albumin (BSA) under ultrasonic irradiation," *Journal of Molecular Catalysis A*, vol. 341, no. 1-2, pp. 89–96, 2011.

[15] P. A. Ramires, A. Romito, F. Cosentino, and E. Milella, "The influence of titania/hydroxyapatite composite coatings on in vitro osteoblasts behaviour," *Biomaterials*, vol. 22, no. 12, pp. 1467–1474, 2001.

[16] A. Bigi, N. Nicoli-Aldini, B. Bracci et al., "In vitro culture of mesenchymal cells onto nanocrystalline hydroxyapatite-coated Ti13Nb13Zr alloy," *Journal of Biomedical Materials Research A*, vol. 82, no. 1, pp. 213–221, 2007.

[17] H. M. Kim, W. Chae, K. Chang et al., "Composite nanofiber mats consisting of hydroxyapatite and titania for biomedical applications," *Journal of Biomedical Materials Research B*, vol. 94, no. 2, pp. 380–387, 2010.

[18] S. Tamilselvi, H. B. Raghavendran, P. Srinivasan, and N. Rajendran, "In vitro and in vivo studies of alkali- and heat-treated Ti-6Al-7Nb and Ti-5Al-2Nb-1Ta alloys for orthopedic implants," *Journal of Biomedical Materials Research A*, vol. 90, no. 2, pp. 380–386, 2009.

[19] A. Mello, Z. Hong, A. M. Rossi et al., "Osteoblast proliferation on hydroxyapatite thin coatings produced by right angle magnetron sputtering," *Biomedical Materials*, vol. 2, no. 2, pp. 67–77, 2007.

[20] H. Daugaard, B. Elmengaard, J. E. Bechtold, T. Jensen, and K. Soballe, "The effect on bone growth enhancement of implant coatings with hydroxyapatite and collagen deposited electrochemically and by plasma spray," *Journal of Biomedical Materials Research A*, vol. 92, no. 3, pp. 913–921, 2010.

[21] H. Fleisch, "Bisphosphonates: mechanisms of action," *Endocrine Reviews*, vol. 19, no. 1, pp. 80–100, 1998.

[22] R. G. Russell and M. J. Rogers, "Bisphosphonates: from the laboratory to the clinic and back again," *Bone*, vol. 25, no. 1, pp. 97–106, 1999.

[23] D. L. Douglas, T. Duckworth, and R. G. Russell, "Effect of dichloromethylene diphosphonate in Paget's disease of bone and in hypercalcaemia due to primary hyperparathyroidism or malignant disease," *The Lancet*, vol. 1, no. 8177, pp. 1043–1047, 1980.

[24] G. R. Mundy and T. Yoneda, "Bisphosphonates as anticancer drugs," *New England Journal of Medicine*, vol. 339, no. 6, pp. 398–400, 1998.

[25] D. E. Hughes, B. R. MacDonald, R. G. G. Russell, and M. Gowen, "Inhibition of osteoclast-like cell formation by bisphosphonates in long-term cultures of human bone marrow," *Journal of Clinical Investigation*, vol. 83, no. 6, pp. 1930–1935, 1989.

[26] A. Carano, S. L. Teitelbaum, J. D. Konsek, P. H. Schlesinger, and H. C. Blair, "Bisphosphonates directly inhibit the bone resorption activity of isolated avian osteoclasts in vitro," *Journal of Clinical Investigation*, vol. 85, no. 2, pp. 456–461, 1990.

[27] M. Yoshinari, Y. Oda, H. Ueki, and S. Yokose, "Immobilization of bisphosphonates on surface modified titanium," *Biomaterials*, vol. 22, no. 7, pp. 709–715, 2001.

[28] H. Kajiwara, T. Yamaza, M. Yoshinari et al., "The bisphosphonate pamidronate on the surface of titanium stimulates bone

formation around tibial implants in rats," *Biomaterials*, vol. 26, no. 6, pp. 581–587, 2005.

[29] T. H. Koo, J. S. Borah, Z. C. Xing, S. M. Moon, Y. Jeong, and I. K. Kang, "Immobilization of pamidronic acids on the nanotube surface of titanium discs and their interaction with bone cells," *Nanoscale Research Letters*, vol. 8, no. 1, p. 124, 2013.

[30] K. H. Lee, H. Y. Kim, Y. J. Ryu, K. W. Kim, and S. W. Choi, "Mechanical behavior of electrospun fiber mats of poly(vinyl chloride)/polyurethane polyblends," *Journal of Polymer Science B*, vol. 41, no. 11, pp. 1256–1262, 2003.

[31] K. W. Muszynski, F. W. Ruscetti, J. M. Gooya, D. M. Linnekin, and J. R. Keller, "Raf-1 protein is required for growth factor-induced proliferation of primitive hematopoietic progenitors stimulated with synergistic combinations of cytokines," *Stem Cells*, vol. 15, no. 1, pp. 63–72, 1997.

[32] C. D. Wagner, W. M. Riggs, L. E. Davis, and J. F. Moulder, *Handbook of X-Ray Photoelectron Spectroscopy*, Perkin-Elmer Corporation Muilenberg, Minnesota, Minn, USA, 1979.

[33] E. R. Van Beek, L. H. Cohen, I. M. Leroy, F. H. Ebetino, C. W. G. M. Löwik, and S. E. Papapoulos, "Differentiating the mechanisms of antiresorptive action of nitrogen containing bisphosphonates," *Bone*, vol. 33, no. 5, pp. 805–811, 2003.